New Phytologist

Phytophthora infestans RXLR effector PITG20303 targets a potato MKK1 protein to suppress plant immunity

Yu Du[1]* (ID), Xiaokang Chen[1]*, Yalu Guo[1]*, Xiaojiang Zhang[1], Houxiao Zhang[1], Fangfang Li[1], Guiyan Huang[2,3], Yuling Meng[4] and Weixing Shan[4] (ID)

[1]State Key Laboratory of Crop Stress Biology for Arid Areas and College of Horticulture, Northwest A&F University, Yangling, Shaanxi 712100, China; [2]State Key Laboratory of Crop Stress Biology for Arid Areas and College of Agronomy, Northwest A&F University, Yangling, Shaanxi 712100, China; [3]College of Life Sciences, Northwest A&F University, Yangling, Shaanxi 712100, China; [4]China–USA Citrus Huanglongbing Joint Laboratory, National Navel Orange Engineering Research Center, College of Life Sciences, Gannan Normal University, Ganzhou 341000, China

Summary

- Pathogens secret a plethora of effectors into the host cell to modulate plant immunity. Analysing the role of effectors in altering the function of their host target proteins will reveal critical components of the plant immune system.
- Here we show that *Phytophthora infestans* RXLR effector PITG20303, a virulent variant of AVRblb2 (PITG20300) that escapes recognition by the resistance protein Rpi-blb2, suppresses PAMP-triggered immunity (PTI) and promotes pathogen colonization by targeting and stabilizing a potato MAPK cascade protein, StMKK1. Both PITG20300 and PITG20303 target StMKK1, as confirmed by multiple *in vivo* and *in vitro* assays, and *StMKK1* was shown to be a negative regulator of plant immunity, as determined by overexpression and gene silencing.
- *StMKK1* is a negative regulator of plant PTI, and the kinase activities of StMKK1 are required for its suppression of PTI and effector interaction. PITG20303 depends partially on MKK1, PITG20300 does not depend on MKK1 for suppression of PTI-induced reactive oxygen species burst, while the full virulence activities of nuclear targeted PITG20303 and PITG20300 are dependent on MKK1.
- Our results show that PITG20303 and PITG20300 target and stabilize the plant MAPK cascade signalling protein StMKK1 to negatively regulate plant PTI response.

Introduction

Phytophthora infestans is a notorious oomycete plant pathogen, which causes late blight on potato and tomato and is a serious threat to food security. To enable infection it secrets a plethora of effectors into host cells to modulate the host immune response and facilitate infection (Haas *et al.*, 2009). RXLR effectors belong to the largest group of effectors, are only found in oomycete pathogens and are defined by a conserved Arg-X-Leu-Arg (RXLR) motif at their N-terminus. The RXLR motif is required for effector host translocation (Kale *et al.*, 2010). RXLR effectors exploit diverse machineries to manipulate plant cellular processes; for example, they inhibit plant endoplasmic reticulum (ER)-stress-mediated immunity (Fan *et al.*, 2018), disturb plant PTI (PAMP-triggered immunity) responses (Bouwmeester *et al.*, 2011; Zheng *et al.*, 2018), target plant defence negative regulators (Wang *et al.*, 2015; Boevink *et al.*, 2016; Yang *et al.*, 2016; He *et al.*, 2018), suppress host cell death (Jing *et al.*, 2016), interfere with protein secretion (Bozkurt *et al.*, 2011; Du *et al.*, 2015a; Tomczynska *et al.*, 2018), interfere with the plant RNA silencing

process (Qiao *et al.*, 2015; Vetukuri *et al.*, 2017) and regulate plant transcription (Mclellan *et al.*, 2013; Kong *et al.*, 2017; Turnbull *et al.*, 2017).

Plants have evolved multilayered immune systems to recognize and combat pathogens. The first layer of plant defence is the plasma membrane-localized pattern recognition receptors (PRRs), which detect the conserved molecules of microbes known as pathogen/microbe-associated molecular patterns (PAMPs/MAMPs) (Jones & Dangl, 2006; Zipfel, 2008), and thus activate PTI. As a consequence, pathogens have evolved a plethora of small-secreted effectors to interfere with plant PTI responses, leading to effector-triggered susceptibility. To combat the role of the effectors, a second layer of plant defence is conferred by intercellular nucleotide-binding leucine-rich repeat receptors (NLRs) known as resistance proteins, which recognize the presence of specific pathogen effectors and activate effector-triggered immunity (ETI) (Hardham & Cahill, 2010; Du *et al.*, 2015b).

Upon PTI activation, plasma membrane-localized PRRs sense the pathogen PAMPs or MAMPs and activate MAPK (mitogen activated protein kinase) cascades to signal to the nucleus to activate an immune response (Ingle *et al.*, 2006). MAPK cascades

*These authors contributed equally to this work.

contain an MAPK kinase kinase (MAPKKK, MEKK or MAP3K), an MAPK kinase (MAPKK, MEK or MAP2K) and an MAPK. Upon PTI response, the MAPKKKs are activated and phosphorylated MKKs that then phosphorylate MAPKs. At least two MAPK cascades that consist of MEKK1-MKK4/5-MPK3/6 and MEKK1-MKK1/2-MPK4 are activated during the flg22-triggered PTI response (Zhang *et al.*, 2017). The role of MPK cascade proteins in plant immunity is subtle with different experimental approaches suggesting differing outcomes. For example, MPK4 was previously shown to positively regulate plant immunity and was phosphorylated by MKK1/2 (Zhang *et al.*, 2012; Zhang *et al.*, 2017). However, the constitutively active MPK4 was shown to negatively regulate plant immunity (Berriri *et al.*, 2012), and MPK4 was also shown to phosphorylate ASR3 to repress flg22-induced gene expression (Li *et al.*, 2015).

MAPK signalling components have been shown to be common targets of bacterial pathogen effectors targets (Bi & Zhou, 2017). Many bacterial effectors are reported to target the flg22-activated MAPK cascade proteins to inhibit plant PTI response (Zhang *et al.*, 2007, 2012; Ling *et al.*, 2017). They either manipulate MAPKKKs or proteins upstream of MAPKKKs to disturb PRR-mediated resistance (He *et al.*, 2006; Zhang *et al.*, 2010; Feng *et al.*, 2012; Li *et al.*, 2016), or directly target and suppress the activity of MAPKKK downstream signalling components MAPKK or MAPK (Wang *et al.*, 2010; Cui *et al.*, 2010; Eschen-Lippold *et al.*, 2016; Teper *et al.*, 2018). For instance, *Pseudomonas syringae* type III effector HopB1 and HopF2 perturb plant PTI upstream of MAPKKK by targeting BAK1 (Zhou *et al.*, 2014; Li *et al.*, 2016), AvrPphB inhibits PTI via cleaving PBL kinases (Zhang *et al.*, 2010), and the *Xanthomonas campestris* type III effector AvrAC enhances pathogen virulence by targeting and inhibiting the activities of BIK1 and RIPK (Feng *et al.*, 2012). The *Xanthomonas euvesicatoria* type III effector XopAU targets and activates MKK2 to promote pathogen disease (Teper *et al.*, 2018) and in *P. syringae* the effector AvrRpt2 represses MPK4/MPK11 activation (Eschen-Lippold *et al.*, 2016), while effectors HopF2 and HopAI1 target and inhibit the kinase activity of AtMKK5 and MPK3/MPK6/MPK4, respectively, to inhibit PTI (Zhang *et al.*, 2007; Wang *et al.*, 2010; Zhang *et al.*, 2012). Recently, it has been shown that tomato yellow leaf curl China virus betasatellite protein βC1 targets and inhibits the kinase activities of MKK2 and MPK4 to counter host defence (Hu *et al.*, 2019).

Several oomycete RXLR effectors have been reported to suppress plant PTI responses (Bos *et al.*, 2010; Saunders *et al.*, 2012; Dagdas *et al.*, 2016; Zheng *et al.*, 2018). However, few of them are known to target MAPKKKs and interfere with MAPK signalling; for example, the *P. infestans* RXLR effectors Pi22926, PexRD2 and Pi17316 were found to target host StMAP3Kβ2, MAPKKKε and MAP3K StVIK, respectively (King *et al.*, 2014; Murphy *et al.*, 2018; Ren *et al.*, 2019). *P. sojae* Avh331 was shown to inhibit the MAPK signalling pathway, but no physical association of Avh331 and MAPK signalling proteins was demonstrated (Cheng *et al.*, 2012).

The *P. infestans* RXLR effector PITG20303 is a virulent variant of AVRblb2 (PITG20300), harbouring an amino acid alteration from Ala/Ile/Val to Phe at position 69, enabling it to escape recognition by the broad-spectrum resistance protein Rpi-blb2 (Vleeshouwers *et al.*, 2011; Oliva *et al.*, 2015; Haverkort *et al.*, 2016). The AVRblb2 effector family contains four potential variants and different numbers are present in different *P. infestans* isolates, which implies an important role in pathogenicity and that variants may evade recognition by RPI-blb2 or manipulate different host targets. PITG20303 was found to localize in the host nucleus and more weakly in the plasma membrane to interfere with the plant PTI response and promote *P. infestans* colonization (Zheng *et al.*, 2014). By contrast, PITG20300 (AVRblb2) localizes to the host plasma membrane and prevents the secretion of a cysteine proteinase C14 to the apoplast (Bozkurt *et al.*, 2011). Thus, we hypothesize that PITG20303 utilizes a different virulence mechanism from that reported for PITG20300. Here we show that both PITG20303 and PITG20300 suppress the plant PTI response and target a potato StMKK1 protein. Silencing and overexpression experiments show that *StMKK1* negatively regulates plant PTI. The kinase activity of StMKK1 is required for its negative regulation of plant defence and effector interaction. StMKK1 is largely dependent on PITG20303 for its virulence activity, and it is fully required for the virulence activity of the nuclear targeted PITG20303NLS and PITG20300NLS. Thus, we propose that the *P. infestans* RXLR effectors PITG20303 and PITG20300 target and stabilize a plant resistance-negative regulator StMKK1 to suppress plant immunity.

Materials and Methods

Plasmid construction

For yeast two-hybrid (Y2H) assays, *PITG20303* was cloned into the pGBKT7 vector using *Eco*RI and *Bam*HI sites to form the bait plasmid BD-20303. StMKK1 (Sotub12g010200) was amplified from cDNA generated from potato cultivar Qingshu9, and cloned into the pGADT7 vector using *Eco*RI and *Bam*HI sites to form the AD-StMKK1 plasmid. The plasmids used for co-immunoprecipitation (Co-IP) assays were generated by cloning of *PITG20303* or *PITG04097* genes under control of the 35S promoter in the pART27-N7myc vector (Fan *et al.*, 2018) using *Eco*RI and *Xba*I sites to form myc-20303 and myc-04097 plasmids. StMKK1 was fused to greem fluorescent protein (GFP) by cloning into the pART27-NGFP vector (Fan *et al.*, 2018) using *Eco*RI and *Xba*I sites to form the GFP-StMKK1 plasmids. For firefly luciferase complementation imaging (LCI) assays, *StMKK1* and *PITG20303* were cloned into pCAMBIA-NLuc and pCAMBIA-CLuc (Chen *et al.*, 2008) using *Kpn*1 and *Sal*1 sites to form the StMKK1-nluc and cluc-20303 plasmids, respectively. For bimolecular fluorescence complementation (BiFC) assays, *StMKK1* was cloned into pDEST-VYCE(R)^GW vector using *Stu*I and *Kpn*I sites to form the YC-StMKK1 plasmid. *PITG20303*, *PITG04097* and *PITG20300* were cloned into pDEST-VYNE(R)^GW vector using *Spe*I and *Xho*I sites to form the YN-20303, YN-04097 and YN-20300 plasmids, respectively. To generate the YN-AVR3a plasmid, *PiAVR3a* was

cloned into pDEST-VYNE(R)^{GW} vector using *Stu*I and *Kpn*I sites. To generate the cluc-20303 and StMKK1-nluc plasmids, *PITG20303* and *StMKK1* were cloned into pCAMBIA1300 vector using *Kpn*1 and *Sa*L1 sites. For colocalization assays, GFP-20303, GFP-20300, mCherry-20303, mCherry-20300 and mCherry plasmids were generated in a similar way using *Eco*R1 and *Xba*I sites into pART27-NGFP and pART27-NmCherry vectors (Fan *et al.*, 2018), respectively. For *in vitro* kinase activity assays, GFP, StMKK1 or StMKK1^{K99M} were cloned into pET32a vector using *Nco*I and *Xho*I sites to make His-GFP, His-StMKK1 and His-StMKK1^{K99M} plasmids. StMPK4 (Sotub08g028940.1.1) was amplified from cDNA generated from potato cultivar Tianshu11, and cloned into pGEX-6P-1 vector using *Bam*HI and *Sal*I sites to form the GST-StMPK4 plasmid. All the fragments for cloning and all the point mutations were PCR-generated and the relevant primers are listed in Supporting Information Table S1.

Plant growth conditions and pathogen infection assays

Nicotiana benthamiana plants were grown under standard glasshouse conditions. Five-week-old plants were used for infection assays. *P. infestans* isolate 14-3-GFP was grown on rye Suc agar plates at 16–18°C for 9–12 d before zoospores were harvested and used for infection. *Phytophthora parasitica* was cultured as described by Fan *et al.* (2018). Infection assays were performed according to Champouret *et al.* (2009). Pathogen-inoculated leaves were kept under moisture at 18°C for 5 or 6 d for *P. infestans* and at 23°C for 2 or 3 d for *P. parasitica* before lesion diameters were measured.

Agroinfiltration and VIGS

Agrobacterium tumefaciens strain C58C1 carrying binary transformation vectors was grown in liquid LB medium with appropriate antibiotics at 28°C for 2 d before centrifugation and resuspension in infiltration medium as described (Champouret *et al.*, 2009). The *Agrobacterium* suspensions were adjusted to an OD$_{600}$ of 0.1 for confocal microscope and BiFC assays and 0.3 for Co-IP and infection assays. For coexpression assays, *Agrobacterium* cultures carrying different vectors were mixed in a 1 : 1 ratio before infiltration.

For selection of target sequence for virus-induced gene silencing (VIGS), we mined the MKK1/2 protein sequences in the Sol genomics network database (https://solgenomics.net/), and identified four genes encoding *MKK1* in *N. benthamiana*. We selected two cDNA fragments: MKK*seq1* targets two highly conserved genes *Niben101Scf10103g03014* and *Niben101Scf00611 G07010*, and MKK*seq2* targets *Niben101Scf02790g03012* and *Niben101Scf13387g00027*. We fused these fragments to form the TRV-*NbMKK1* construct. The sequence alignment is shown in Fig. S6. TRV-*GUS* was used as a control (Tameling & Baulcombe, 2007). The primers used in this assay are shown in Table S1. *Agrobacterium* cultures containing TRV2 and TRV1 mixed in a 1 : 1 ratio with an OD$_{600}$ of 1 were infiltrated into the first two leaves of 2-wk-old *N. benthamiana*. The fifth and sixth leaves from the bottom were used for infection assays at 3 wk after VIGS inoculation.

flg22 treatments and ROS production

Leaves from 4-wk-old *N. benthamiana* plants were infiltrated with 10 µM flg22 solution. Samples for quantitative reverse transcriptase PCR (qRT-PCR) were collected at 3 h after flg22 treatment. Analysis of reactive oxygen species (ROS) production was performed according to Li *et al.* (2016).

Gene expression assay

Total RNA was extracted using TRIzol reagent (Invitrogen). First-strand cDNA was synthesized using 1 µg of RNA by using the PrimeScript RT reagent Kit (TaKaRa, Shiga, Japan) according to the manufacturer's instructions. The cDNA was diluted 20 times and 5 µl of the diluted cDNA was used as template per PCR with SYBR Green master mix (Roche). qRT-PCR was run on a iQ7 Real-Time Cycler (Life Technologies). Gene expression was quantified using the Delta Delta Ct method and normalized to the housekeeping gene *actin* for *N. benthamiana*. To assess gene silencing efficiency, primer pairs were designed beyond the VIGS-targeted sequence (Table S1).

Co-immunoprecipitation and Western blot analysis

Agroinfiltrated *N. benthamiana* leaves were harvested at 2 d post agroinfiltration (dpi) and used for total protein extraction. GTEN buffer (10% glycerol, 25 mM Tris pH 7.5, 150 mM NaCl, 1 mM EDTA) with 1× protease inhibitor cocktail (Sigma) and 1% Nonidet P-40 (Igepal CA-630) were used for protein extraction. For Co-IP assays, 15 µl of GFP-trap_A beads (Chromotek, Martinsried, Germany) was added to 1.6 ml of total protein extract, and the mixtures were incubated at 4°C for 2 h. Subsequently, the mixtures were spun down at 4°C and the proteins attached to the beads were collected and washed several times. Finally, 100 µl of protein complex solutions was boiled with loading buffer (300 mM Tris-HCl, pH 6.8, 8.7% SDS, 5% β-mercaptoethanol, 30% glycerol and 0.12 mg ml^{-1} bromophenol blue) for 5–10 min.

For protein stability assays, 1 mg MG132 was dissolved in 0.1 ml DMSO, and then distilled H$_2$O (dH$_2$O) was used to bring the volume to 21 ml to obtain a concentration of 100 µM. For control treatments, 0.1 ml DMSO was diluted to a volume of 21 ml using dH$_2$O. *Myc-StMKK1* was co-agroinfiltrated with *GFP-20303*, *GFP-20300* or *GFP* into *N. benthamiana* leaves; 36 h after agroinfiltration, the MG132 or its solvent DMSO solutions were infiltrated to the leaves; and at 48 h after agroinfiltration, leaves were harvested and used for protein isolation and Western blot analysis. For Western blot analysis, proteins were separated on SDS-PAGE gel and then transferred to an Immune-Blot PVDF membrane (Roche). The membranes were then blocked in TBST blocking buffer (pH 7.2, TBS, 0.05% Tween 20 (Sigma)) with 5% nonfat dry milk with gentle shaking at room temperature for

1.5 h. Specific antibodies anti-GFP (#AE012; ABclonal, Wuhan, China), anti-myc (#AE010; ABclonal) or anti-mCherry monoclonal antibody (Abbkine, Wuhan, China) were added into blocking buffer at 1 : 2000 dilution. Membranes were incubated with antibodies for 1.5 h at room temperature with gentle shaking. Subsequently the membranes were washed five times and then incubated with appropriate secondary antibodies of the same dilution. The secondary antibodies used were HRP goat anti-mouse IgG (H + L) antibody (#AS013; ABclonal) and HRP goat anti-rabbit IgG (H + L) antibody (#AS014; ABclonal). Protein bands were detected using an eECL Western blot kit (CWBio, Beijing, China).

The plasma membrane and nuclear proteins were isolated using the plant plasma membrane isolation kit (BB-3152-1; BestBio, Shanghai, China) and plant nuclear protein isolation kit (BB-3154-1; BestBio).

Recombinant protein purification and in vitro phosphorylation assays

The constructs of *His-StMKK1*, *His-StMKK1*^{K99M}, *His-GFP* and *GST-StMPK4* were transformed into *Escherichia coli* strain BL21. Proteins were expressed and purified as described by Fan *et al.* (2018). For *in vitro* phosphorylation assays, 2 µg each of His-StMKK1, His-StMKK1^{K99M} or His-GFP were incubated with 2 µg GST-StMPK4, respectively, in 80 µl reaction buffer, according to the method described by Li *et al.* (2014). The phosphorylation of StMPK4 was detected using anti-pERK antibodies (#4370; Cell Signaling, Danvers, MA, USA).

Y2H assays

The AD library plasmids were transformed into *Saccharomyces cerevisiae* strain AH109. The bait plasmid pGBKT7-20303 was transformed into *S. cerevisiae* strain Y187. Yeast mating and Y2H screening were performed according to the Matchmaker GAL4 Two-Hybrid System 3 & Libraries User Manual (Clontech, Palo Alto, CA, USA). For the Y2H assay, pGBKT7 and pGADT7 vectors were cotransformed into the yeast strain AH109. Transformations were checked on SD/-Trp-Leu medium and interactions were confirmed by the gain of α-galactosidase (α-gal) activity. Yeast controls showing interaction and no interaction were provided by the Matchmaker GAL4 Two-Hybrid System 3 (Clontech).

Confocal microscopy

For BiFC and protein subcellular localization assays, an Olympus IX83 confocal microscope (Tokyo, Japan) was used. The excitation wavelengths used for Venus and GFP were 514 and 488 nm, respectively, and their emissions were detected between 500 and 540 nm. The mCherry fluorescence was excited at 559 nm wavelength and specific emissions between 600 and 680 nm were collected. The subsequent image processing and Figure generation were conducted with Olympus Fluoview and Adobe Illustrator.

Accession numbers

Accession numbers are as follows: AtMKK1, AT4G26070; AtMKK2, AT4G29810; SlMKK1/2, Solyc12g009020; StMKK1, Sotub12g010200; NbMKK1/2, Niben101Scf10103g03014, Niben101Scf00611g07010, Niben101Scf02790g03012, Niben 101Scf13387g00027.

Results

P. infestans effector PITG20303 promotes pathogen colonization

To investigate whether PITG20303 is a virulence effector that promotes *P. infestans* colonization *in planta*, *GFP-PITG20303* and the control *GFP-GUS* were transiently expressed into *N. benthamiana* leaves and subsequently used for infection assays. The results demonstrate that PITG20303 significantly promotes *P. infestans* colonization at 5 d after inoculation (dai) (Fig. 1). To investigate if PITG20303 also promotes other *Phytophthora* pathogen colonization, we inoculated GFP-PITG20303 and GFP-GUS expressed leaves with *P. parasitica*. The results showed that PITG20303 significantly promotes *P. parasitica* colonization at 3 dai (Fig. S1). The expression of GFP-PITG20303 and GFP-GUS were confirmed by Western blot (Fig. S1d).

In a previous report, PITG20300 was shown to localize to the plasma membrane and partially to the nucleus (Bozkurt *et al.*, 2011), while its virulent allele PITG20303 appeared to localize in the nucleus and the cytoplasm (Zheng *et al.*, 2014). To confirm this, we co-agroinfiltrated *GFP-PITG20303*, *GFP-PITG20300* and the control *GFP* with the plasma membrane marker myr-mCherry (a myristoylation site fused to the N-terminus of mCherry) and the nuclear marker H2B-mCherry (Long *et al.*, 2019) into *N. benthamiana* leaves, respectively. Subcellular localization was examined using confocal microscopy. GFP-PITG20303 was observed in the nucleus and the signals overlapped with H2B-mCherry in the nucleus; some weak signals were also found on the plasma membrane that overlapped with myr-mCherry (Fig. S2). GFP-PITG20300 localizes mainly on the plasma membrane and weakly in the nucleus; we observed the signals nicely overlapped with myr-mCherry on the plasma membrane and weakly with H2B-mCherry in the nucleus. Stable expression of the fusion proteins was confirmed by Western blot, and the ratios of plasma membrane/nuclear proteins of two effectors were confirmed by isolation of plasma membrane and nuclear proteins (Fig. S3). The results showed that PITG20303 and PITG20300 all localize to the plasma membrane and nucleus. However, for PITG20303 the proportion of nuclear- and plasma membrane-localized proteins was similar, about 50% each, while about 80% of PITG20300 is localized on the plasma membrane and only 16% localized inside the nucleus (Fig. S3). The plasma membrane and nuclear markers show solely localization either on the plasma membrane or inside the nucleus.

To investigate which subcellular localization is required for the virulence activity of PITG20303, we fused a myristoylation site (myr) to the N-terminus of GFP-20303, and nuclear export
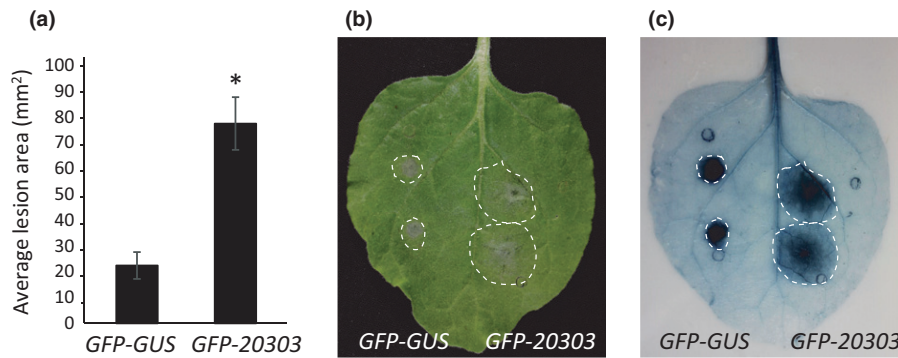
Fig. 1 Transient expression of *Phytophthora infestans* RXLR effector Avrblb2 variant PITG20303 in *Nicotiana benthamiana* promotes plant susceptibility to *P. infestans*. (a) *Agrobacterium tumefaciens* cells carrying control *GFP-GUS* were infiltrated into the left panel of the leaf, while cells carrying *GFP-PITG20303* were infiltrated into the right panel of the same leaf. Zoospores of *P. infestans* isolate 14-3-GFP were inoculated onto the agroinfiltrated leaves at 1 d post-infiltration (dpi), and lesion diameters were measured and lesion areas were scored at 5 d after infection (dai). Bars show the mean lesion areas. Error bars show SE from 12 replicates. Asterisks indicate significant differences ($n \geq 12$; one-sided Student's t-test, $P \leq 0.01$). (b) Lesion development was photographed at 5 dai, and lesion areas are indicated with dotted circles. (c) Trypan blue staining of the lesions. The experiments were repeated more than three times with similar results.

(NES) and nuclear import (NLS) signals to the C-terminus of GFP-20303. We transiently expressed *Myr-GFP-20303*, *GFP-PITG20303NES* and *GFP-PITG20303NLS* in *N. benthamiana* leaves, and confocal microscopy results showed that the myristoylation sites target GFP-20303 to the plasma membrane, the NES signal targets GFP-20303 outside the nucleus, and the NLS signal targets GFP-20303 mainly inside the nucleus as expected (Fig. S4a). We then tested the functions of *Myr-GFP-20303*, *GFP-PITG20303NES* and *GFP-PITG20303NLS* in *P. infestans* colonization using detached leaf assays. The results showed that either plasma membrane (myr- or NES-fusion proteins) or nuclear-localized PITG20303 (NLS-fusion protein) all promoted *P. infestans* colonization (Fig. S4b–d). The integrity of fusion proteins is shown by Western blots in Fig. S4(e).

Both PiPITG20303 and PiPITG20300 target a potato StMKK1 protein

To explore the molecular mechanism of PITG20303 in host defence suppression, we identified its host targets by Y2H screening. We constructed a prey library from a combination of RNA prepared at 0 and 12 h after *P. infestans* infection of a compatible tomato cultivar Moneymaker. Using PITG20303 as the bait to screen against this prey library, we identified several PITG20303-interacting candidate proteins. After a one to one Y2H confirmation of interaction, and functional analysis of targets in plant immunity, MKK1 was selected as a candidate target. To confirm the interaction between PITG20303 and MKK1, we cloned the full-length potato *StMKK1* and tomato *SlMKK1* from the potato cultivar Qingshu9 and the tomato cultivar Moneymaker, respectively. A pairwise Y2H assay was performed using PITG20303 as bait and StMKK1 as prey with empty vector as negative control. The results confirmed that both PITG20303 and PITG20300 interact with StMKK1 and SlMKK1 in yeast cells (Fig. 2a; Fig. S5a). Their *in planta* specific interaction was further confirmed by Co-IP assays. The results show that both myc-PITG20303 and myc-PITG20300 interact with StMKK1 in Co-

IP assays (Fig. 2b). We also performed firefly LCI assays to confirm the interaction. The combination of GmBZR2 and PP2C was used as a positive control (Lu *et al.*, 2017). The results showed that the combination of StMKK1-nluc with cluc-20303 or cluc-20300 restored the catalytic activity of luciferase even more strongly than that of the positive control (Figs 2c, S5b). The interaction of NbMKK1 with PITG20303 or PITG20300 was also found in Co-IP assays (Fig. S5c). To determine the subcellular localization of the PITG20303 and StMKK1 interaction, we performed a BiFC assay. N-terminal half yellow fluorescent protein (YFP) (YN) fused *PITG20303* and *PITG20300* were co-agroinfiltrated with C-terminal half YFP (YC) fused *StMKK1* into *N. benthamiana* leaves and *YN-PITG04097* and *YN-AVR3a* were co-expressed with *YC-StMKK1* as controls. The results showed that PITG20303 interacts with StMKK1 in the host nucleus, while PITG20300 and the negative controls PITG04097 and AVR3a do not (Fig. 2d). The expression of YN- and YC-fusion proteins used in BiFC assays was determined by western blots using appropriate antibodies (Fig. S5d).

To confirm the subcellular localization of StMKK1 and PITG20303, we performed co-localization assays by co-expressing *GFP-StMKK1* with *mCherry-PITG20303*, *mCherry-PITG20300* and untagged *mCherry*, respectively, in *N. benthamiana* leaves. The results showed that mCherry-PITG20300 localizes on the plasma membrane and weakly in the nucleus, while mCherry-20303 localizes in the nucleus and on the plasma membrane. Fluorescence of GFP-StMKK1 was predominantly in the cytoplasm and nucleus, and overlapped with free mCherry in the cytoplasm and nucleus and with mCherry-20303 in the nucleus only (Fig. S6a,b). The fluorescence of GFP-StMKK1 weakly overlapped with mCherry-PITG20300 in the nucleus. Together, the results showed that both effectors PITG20303 and PITG20300 associate with StMKK1 in the host nucleus, but with different intensities. The expression of GFP- and mCherry-fusion proteins used in co-localization assays was determined by Western blots using appropriate antibodies (Fig. S6c).
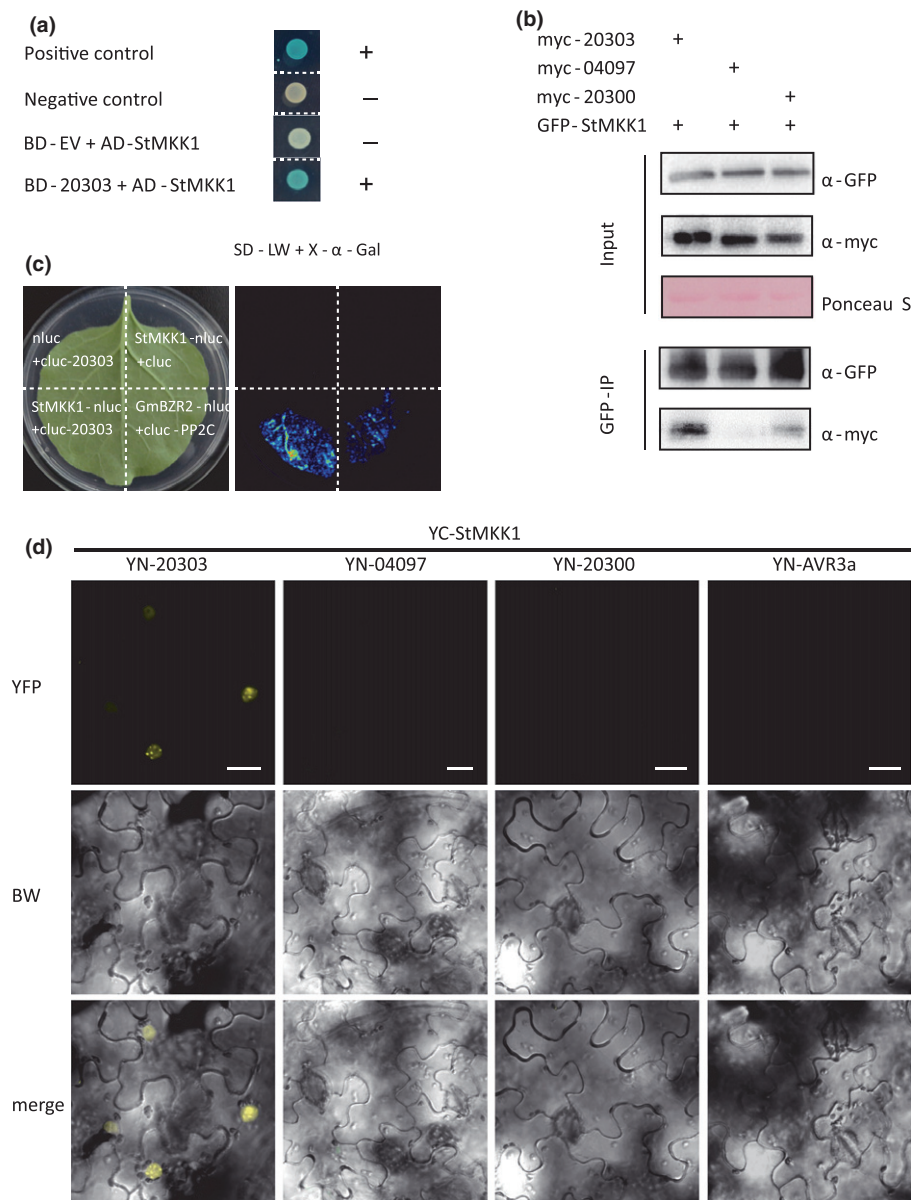
Fig. 2 PITG20303 targets a potato StMKK1 protein. (a) Yeast co-expressing PITG20303 and StMKK1 were grown on SD-LW medium and yielded α-galactosidase activity while the empty vector control (EV) with StMKK1 did not. (b) Co-immunoprecipitation (Co-IP) was performed using GFP-Trap and confirmed that GFP-tagged StMKK1 associated with myc-20303 and myc-20300, but not with the myc-04097 control. +, expression of proteins in the leaves. Protein loading is indicated by Ponceau stain (Ponceau S). (c) The leaf picture on the left shows the infiltration of constructs used in the luciferase complementation assays. The fluorescence signal in the right-hand image shows the protein-protein interaction. The combination of GmBZR2-nluc with cluc-PP2c was used as a positive control. (d) BiFC assay confirming that PITG20303 interacts with StMKK1 in the nucleus of the plant. We fused the C-terminus of YFP (YC) to the N-terminus of StMKK1, and the N-terminus of YFP (YN) to the N terminus of PITG20303, PITG04097, PITG20300 and AVR3a. YC-StMKK1 was co-agroinfiltrated with YN-20303, YN-04097, YN-20300 and YN-AVR3a into *Nicotiana benthamiana* leaves for 2 d before confocal images were taken. Bars, 20 μm.

StMKK1 is a negative regulator of plant immunity

To study the function of *StMKK1* in plant defence against *P. infestans*, we transiently expressed *StMKK1* and control *GFP-GUS* into the right and left panels of *N. benthamiana* leaves, and performed infection assays. The results showed that *StMKK1* expression led to significantly larger lesions compared to the control (Fig. 3a–c), indicating that *StMKK1* expression promotes susceptibility and might be targeted by the effector PITG20303

as a susceptibility factor. To further confirm the function of *MKK1*, VIGS was used to reduce the *MKK1* levels in *N. benthamiana* plants. For selection of a target sequence for VIGS, we mined MKK1 and MKK2 protein sequences in the Sol genomics network database (https://solgenomics.net/), and built a phylogenetc tree of the MKK1/2 protein. Phylogenetic analysis revealed that, in contrast to Arabidopsis, which contains the *MKK1* and *MKK2* genes, in Solanaceous plants, tomato and potato contain one copy of *MKK1*, while *N. benthamiana* has
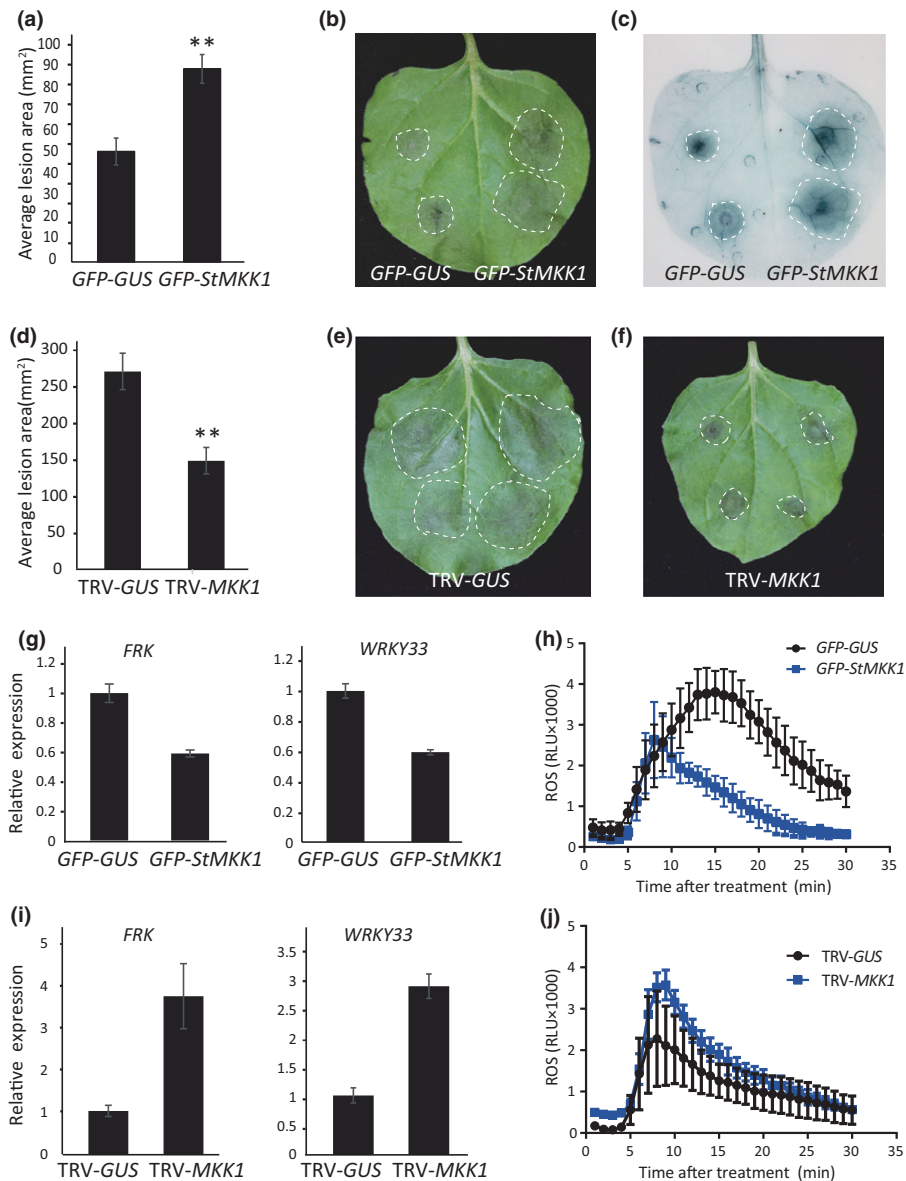
Fig. 3 *StMKK1* negatively regulates plant defence. Average lesion areas on sites expressing either GFP-GUS or GFP-StMKK1 (a), or on TRV-*GUS* and TRV-*MKK1* VIGS plants (d) were measured and calculated at 5 dai. Zoospores from *Phytophthora infestans* isolate 14-3-GFP were used for inoculation. Error bars show SE from more than 10 replicates. Asterisks indicate significant differences ($n \geq 10$; one-sided Student's *t*-test, $P \leq 0.01$). The experiments were repeated four times with similar results. Representative images of GFP-GUS- and GFP-StMKK1-expressing leaves with *P. infestans* lesions before (b) and after (c) trypan blue staining. Representative images of *P. infestans* lesions on TRV-*GUS* (e) and TRV-*MKK1* (f) silenced leaves. qRT-PCR data showing relative expression of the PTI marker genes *FRK* and *WRKY33* in GFP-GUS- and *GFP-StMKK1*-overexpressing leaves (g) and in TRV-*GUS*- and TRV-*MKK*-silenced plant leaves (i). *Nicotiana benthamiana* actin gene expression was used for normalization in qRT-PCR assays. *FRK* and *WRKY33* gene expression levels in *GFP-GUS* or in TRV-*GUS* plants were set to 1. Flg22-induced ROS production in *StMKK1*-overexpressed (h) and *NbMKK1*-silenced plants (j) was analysed. Leaves were treated with 10 µM flg22 before ROS production was measured. RUL, relative luminescence units.

four copies, probably due to its allopolyploid genome (Fig. S7). The sequence alignment of NbMKK1, SlMKK1 and StMKK1 are shown in Fig. S8. The alignment of the silencing sequences and the *NbMKK1* sequences is shown in Fig. S9. Our construct for VIGS was designed to silence all four copies of the *NbMKK1* gene. qRT-PCR analysis showed that all four copies of *NbMKK1* genes were efficiently silenced by the TRV-*MKK1* construct, and no obvious developmental phenotype was observed compared to the control (Fig. S10). TRV-*GUS* and TRV-*NbMKK1* leaves were harvested for detached leaf assays using *P. infestans* isolate

14-3-GFP. The results showed that TRV-*NbMKK1* plants developed significantly smaller lesions compared to the control TRV-*GUS* plants (Fig. 3d–f), further confirming that *MKK1* functions as a negative regulator of plant immunity.

Previous reports show that Arabidopsis *AtMKK1/2* play roles in plant PTI responses. To reveal the role of potato *StMKK1* in the plant PTI response, *StMKK1* was transiently expressed in *N. benthamiana* leaves for 2 d before being treated with the bacterial PAMP flg22. The leaves were then harvested 3 h after flg22 treatment to assess PTI responsive gene expression. The

results showed that the expression of *FRK* and *WRKY33* genes were significantly repressed in *StMKK1*-expressing leaves compared to the control plants (Fig. 3g). Moreover, on *MKK1/2*-silenced *N. benthamiana* plants, upon flg22 treatment the expression of *FRK* and *WRKY33* was induced significantly (Fig. 3i) compared to the control, again indicating its role in the regulation of an early plant PTI response. ROS production was analysed on *MKK1*-overexpressed and *MKK1*-silenced plants. The results showed that on *StMKK1*-overexpressed leaves, flg22-triggered ROS production was reduced to about 60% compared to the control *GFP-GUS* leaves (Fig. 3h). However, ROS production was increased nearly two-fold on TRV-*MKK1* plants compared with the control TRV-*GUS* plants (Fig. 3j). These results indicated that *MKK1* negatively regulates plant PTI responses.

The kinase activity of StMKK1 is required for effector interaction and plant immunity repression

To test whether the functional kinase domain of StMKK1 is necessary for the interaction with the effector PITG20303, we generated two independent mutations that abolish the key residues that are essential for kinase activity of MKK1; that is, the core catalytic arginine (R) and aspartate (D) of the conserved RD kinase motif were substituted to alanine residues, shown as StMKK1^{AA} (StMKK1$^{R191A, D192A}$), and the key lysine (K) was substituted to methionine (M), shown as StMKK1^{K99M}. We also generated a constitutively active phospho-mimicking form of StMKK1^{DE} (StMKK1$^{T220D, T226E}$), via substitution of the conserved Ser/Thr to Asp/Glu residues in the activation loop as described for tobacco and tomato MKK1 (Yang *et al.*, 2001; Li *et al.*, 2014). Co-IP results showed that the kinase-deficient mutation of StMKK1 lost its ability in interaction with the effector PITG20303 and PITG20300 (Fig. 4a,b), while the constitutively active StMKK1^{DE} maintained the interaction with PITG20303 and PITG20300 (Fig. 4c). Effector PITG04097, AVR1-like and GFP-GUS were used as negative controls. Thus, we conclude that the kinase activity of StMKK1 is necessary for the interaction with PITG20303. We subsequently tested StMKK1^{AA}, StMKK1^{K99M} and StMKK1^{DE} in plant defence against *P. infestans* using transient expression assays. The results showed that except for StMKK1^{DE}, all the kinase-deficient mutants lost the ability to promote *P. infestans* colonization (Fig. 4d–e), indicating that StMKK1 requires its kinase activity to promote *P. infestans* infection. The role of StMKK1^{DE} was abolished
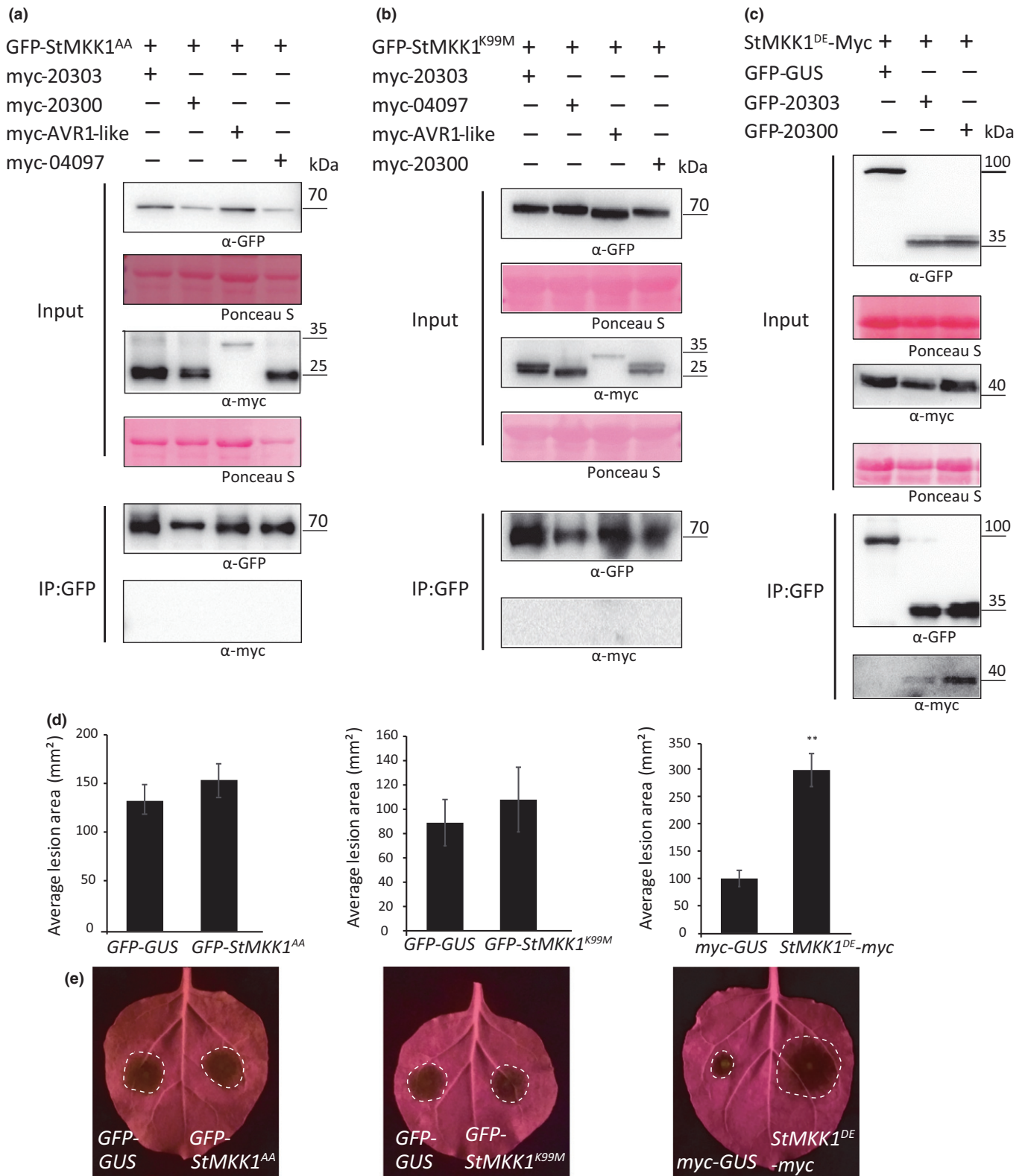
with an N-terminal GFP tag, and thus we used StMKK1^{DE}-myc in the interaction and infection assays. The role of StMKK1, StMKK^{AA} and StMKK1^{K99M} was not affected by N-terminal GFP or C-terminal myc tag. To confirm that StMKK1 has self-phosphorylation activities and the kinase-deficient mutant StMKK1^{K99M} does not, we performed *in vitro* phosphorylation assays as described by Ueno *et al.* (2015). The results showed that His-StMKK1, but not His-StMKK1K99M and control His-GFP, phosphorylates GST-StMPK4, indicating that StMKK1 has self-phosphorylation activity (Fig. S11).

PITG20303 suppresses plant PTI responses and this suppression depends on NbMKK1

To investigate if PITG20303 could suppress the plant PTI response, *GFP-GUS* and *GFP-20303* were transiently expressed into the left and right panels of *N. benthamiana* leaves, respectively. At 2 dpi the transient expressed leaves were then treated with 10 µM flg22 for 3 h before total RNA was isolated. qRT-PCR results showed that *GFP-20303*-expressing leaf halves show a significant reduction in PTI responsive gene expression when compared to the control leaf halves (Fig. 5a). *GFP-GUS*- and *GFP-20303*-expressing leaves were treated with 10 µM flg22 at 2 dpi, and ROS production was analysed. The results showed that ROS production was significantly reduced to 50% in *GFP-20303*-expressing leaves compared to the control *GFP-GUS* (Fig. 5b). These results indicate that the effector PITG20303 could suppress the plant PTI response. The expression of GFP-GUS and GFP-20303 are shown by Western blots in Fig. S12(e).

To investigate if *PITG20303* needs *NbMKK1* to suppress the plant PTI response, we checked the effect of PTI-induced ROS production by *PITG20303* on the *MKK1*-silenced and control plants. GFP and GFP-20303 were transiently expressed into TRV-GUS and TRV-MKK1 plants, and at 2 dpi the leaves were treated with 10 µM flg22 and ROS production was analysed. If PITG20303 depends on NbMKK1 for suppression of PTI, in TRV-MKK1 plants this suppression of ROS production will be compromised. The results showed that in TRV-*GUS* plants, ROS production was significantly reduced to 40% in *GFP-20303*-expressing leaves compared to the control *GFP*-expressing plants. However, in TRV-*MKK1* plants, ROS production was reduced to about 70% in *GFP-20303*-expressing leaves compared to the control (Fig. S12a). This result suggested that effector PITG20303 may partially depend on

Fig. 4 The kinase activity of StMKK1 is required for its interaction with PITG20303 and promotion of *Phytophthora infestans* colonization. (a–c) Co-immunoprecipitation (Co-IP) was performed using GFP-Trap and showed that GFP-tagged StMKK1^{AA} (a) and StMKK1^{K99M} (b) do not associate with myc-20303. (c) StMKK1^{DE}-myc was associated with GFP-20303 but not with the GFP-GUS control. +, expression of proteins in the leaves. Protein loading is indicated by Ponceau stain (Ponceau S). (d, e) GFP- StMKK1^{AA}, GFP-StMKK1^{K99M} or StMKK1^{DE}-myc were agroinfiltrated together with control GFP-GUS or myc-GUS into *Nicotiana benthamiana* leaves as indicated in the images. Zoospores of *P. infestans* isolate 14-3-GFP were inoculated onto the agroinfiltrated leaves at 1 d post-infiltration (dpi), and lesion diameters were measured at 5 d after infection (da)i. (d) Bar graphs showing the mean lesion areas. Error bars show SE from 12 replicates. Asterisks indicate significant differences ($n \geq 12$; one-sided Student's *t*-test, $P \leq 0.01$). (e) Pictures were taken under blue light showing lesion development at 5 dai. Lesion areas are indicated with dotted circles. The experiments were repeated more than three times with similar results.

(a)

GFP-StMKK1^{AA}	+	+	+	+
myc-20303	+	−	−	−
myc-20300	−	+	−	−
myc-AVR1-like	−	−	+	−
myc-04097	−	−	−	+	kDa

(b)

GFP-StMKK1^{K99M}	+	+	+	+
myc-20303	+	−	−	−
myc-04097	−	+	−	−
myc-AVR1-like	−	−	+	−
myc-20300	−	−	−	+	kDa

(c)

StMKK1^{DE}-Myc	+	+	+
GFP-GUS	+	−	−
GFP-20303	−	+	−
GFP-20300	−	−	+	kDa

NbMKK1 in the suppression of the bplant PTI response. Because PITG20303 showed virulence functions when localized on the plasma membrane and nucleus (Fig. S4), we speculate that the effector may has multiple host targets. StMKK1 was shown to localize in the cytoplasm and nucleus, and thus the nuclear-localized PITG20303 may depend largely on StMKK1 for its virulence activity. Thus, we investigated the effect of PTI-induced ROS production by *GFP-20303NLS* on TRV-
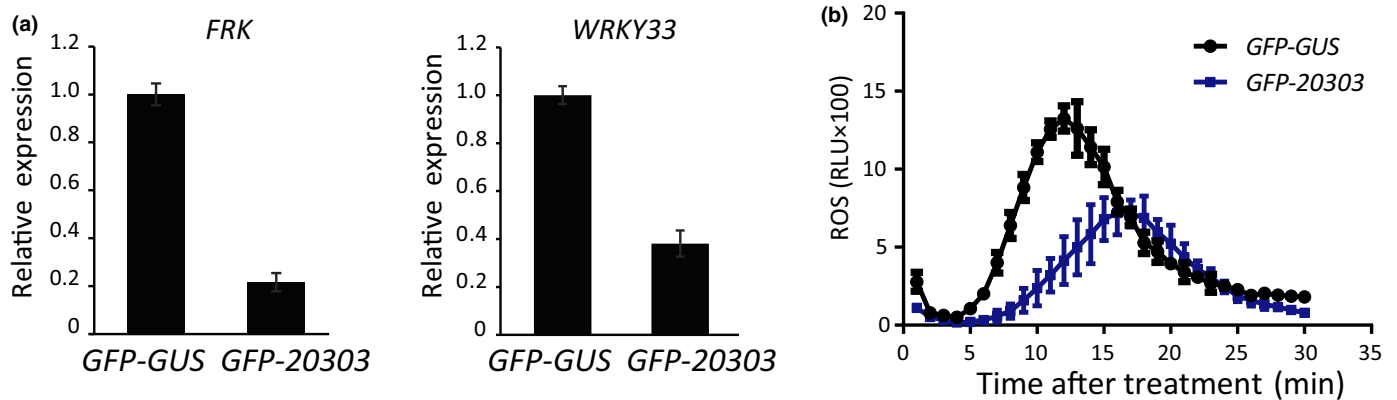
Fig. 5 PITG20303 suppresses the plant PTI response. (a) qRT-PCR data showing relative expression of PTI maker genes *FRK* and *WRKY33* in *GFP-GUS*- and *GFP-20303*-overexpressed leaves. The *Nicotiana benthamiana* actin gene expression was used for normalization in qRT-PCR assays. The relative expression of *FRK* and *WRKY33* is shown on the *y*-axis, and gene expression levels in GFP-20303 were relevant to that in *GFP-GUS* plants. (b) ROS production was measured in *PITG20303*- and *GFP-GUS*-overexpressed leaves after flg22 treatments. Leaves were treated with 10 μM flg22 before ROS production was measured. RUL, relative luminescence units. The experiments were repeated three times with similar results. Error bars show SE from three technical replicates.
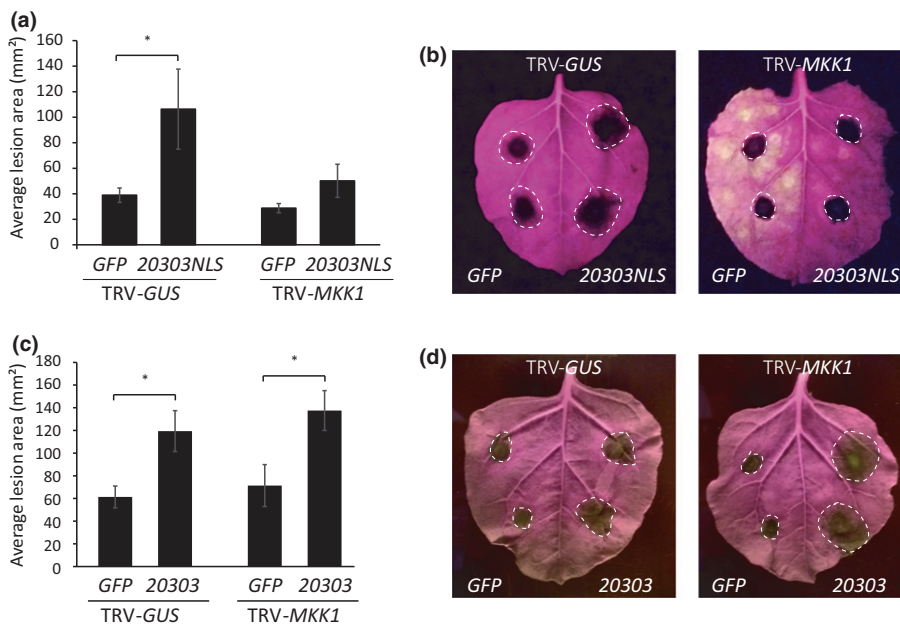

Fig. 6 *GFP-20303NLS* depends on *NbMKK1* in promoting *Phytophthora infestans* colonization. *GFP* and *GFP-20303NLS* (a, b) or *GFP* and *GFP-20303* (c, d) were agroinfiltrated into the left and right panels of TRV-*GUS* and TRV-*MKK1* leaves. Zoospores of *P. infestans* isolate 14-3-GFP were inoculated onto the agroinfiltrated leaves at 1 d post-infiltration (dpi), and lesion diameters were measured at 5 d after infection (dai). (a, c) Bar graphs showing the mean lesion areas. Error bars show SE from 12 replicates. Asterisks indicate significant differences ($n \geq 12$; one-sided Student's *t*-test, $P \leq 0.01$). (b, d) Blue light images showing lesion development at 5 dai. Lesion areas are indicated with dotted circles. The experiments were repeated twice with similar results.

MKK1 plants. The results show that *GFP-20303NLS* supresses ROS production in TRV-*GUS* plants to about 40% compared to the control GFP. However, in TRV-*MKK1* plants, compared to the *GFP* control, *GFP-20303NLS* plants do not supress flg22-triggered ROS production (Fig. S12b). The effects of *GFP-20300* and *GFP-20303NLS* were also checked, and we observed that in both TRV-*GUS* and TRV-*MKK1* plants, GFP-20300 supresses ROS production to a similar level while *GFP-20300NLS* loses its ability to suppress ROS in TRV-*MKK1* plants (Fig. S12c,d).

Together, these results confirm that the nuclear-localized GFP-20303NLS and GFP-20300NLS depend on *MKK1* for their virulence activity. We further used a VIGS assay to examine if *GFP-20303NLS* and *GFP-20303* require *NbMKK1* to promote *P. infestans* colonization. The results showed that in TRV-*GUS* plants, *GFP-20303NLS* and *GFP-20303* significantly promoted *P. infestans* colonization, as shown by larger lesions. However, in TRV-*MKK1* plants, the lesion areas in *GFP*- and *GFP-20303NLS*-expressing sites showed no significant difference, while *GFP-20303*-expressed sites still developed larger lesions (Fig. 6). We also found that the nuclear-targeted PITG20300NLS depends on MKK1 for promotion of *P. infestans* colonization (Fig. S12h). We thus conclude that only the nuclear-localized PITG20303NLS and PITG20300NLS depend on *NbMKK1* for their full virulence activities. Expression of *NbMKK1* in these assays was shown by
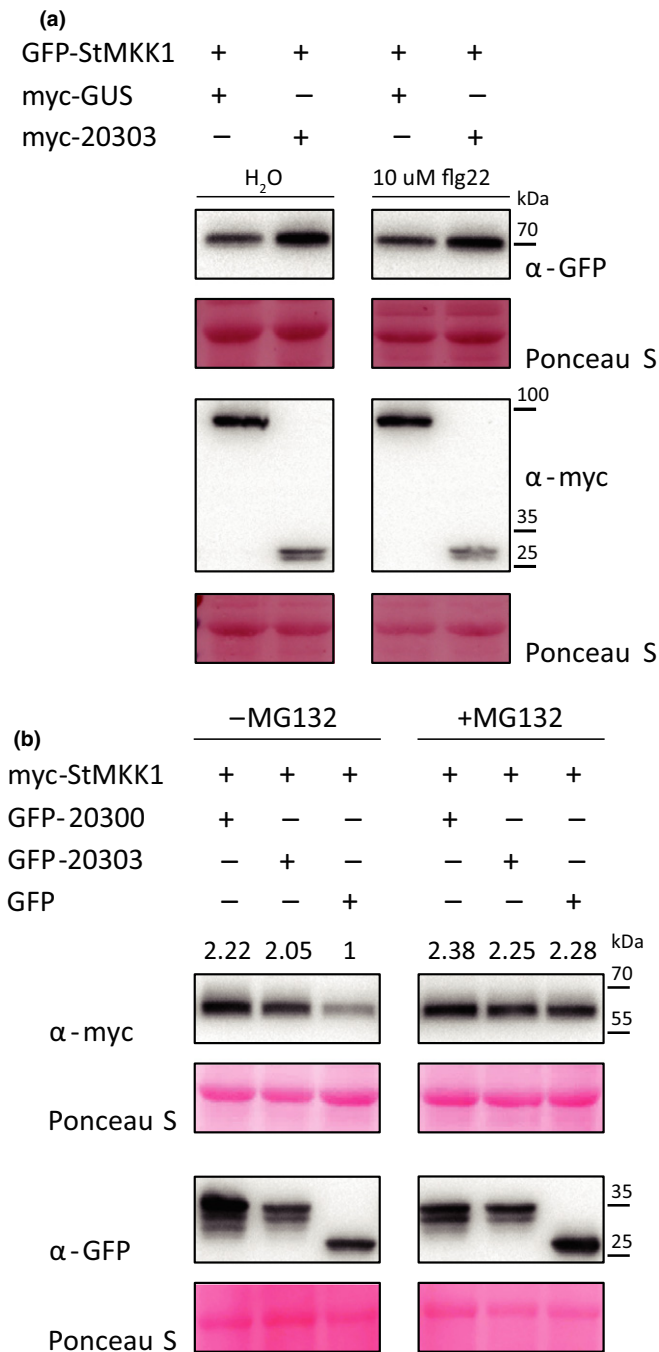
Fig. 7 StMKK1 is stabilized by PITG20303 and PITG20300. (a) Proteins were extracted at 2 d post-infiltration (dpi) from *Nicotiana benthamiana* leaves co-expressing *GFP-StMKK1* and *myc-20303* or *GFP-StMKK1* and *myc-GUS* with and without 10 µM flg22 treatment at 1 dpi. (b) Proteins were extracted at 2 dpi from leaves co-expressing *myc-StMKK1* with *GFP-20300*, *GFP-20303* or *GFP* treated with MG132 or its solvent DMSO at 12 hpi. GFP- and myc-fusion proteins were detected by Western blots with GFP- and myc-antibodies respectively. The experiments were repeated three times with similar results. +, expression of proteins in the leaves. Protein loading is indicated by Ponceau stain (Ponceau S). Numbers indicate the relative intensity of StMKK1 bands normalized to Rubisco.

qRT-PCR (Fig. S12f). Expression of GFP, GFP-20303, GFP-20303NLS, GFP-20300 and GFP-20300NLS is shown by Western blots in Fig. S12(g).

StMKK1 is stabilized by PITG20303 and PITG20300

To test whether the protein accumulation of StMKK1 is altered by effector PITG20303 with and without flg22 treatments, we transiently expressed *GFP-StMKK1* with *myc-20303* and the control *myc-GUS* in the leaves of *N. benthamiana*. Two days after agroinfiltration leaves were harvested for protein isolation. Leaves were treated with 10 µM flg22 or H₂O 24 h before harvest. The results showed that in both flg22-treated and untreated leaves, PITG20303 promoted StMKK1 accumulation compared to the control (Fig. 7a). To investigate whether PITG20303-stabilized StMKK1 is through the 26S proteasome and if PITG20300 stabilizes StMKK1, myc-StMKK1 was co-expressed with GFP-20303, GFP-20300 and GFP in *N. benthamiana* leaves. About 36 h after agroinfiltration, the 26S proteasome inhibitor MG132 or its solvent dimethyl sulfoxide (DMSO) was infiltrated, and 12 h later leaves were harvested for protein isolation. The results showed that both PITG20303 and PITG20300 promote StMKK1 accumulation in the absence of MG132, while in the presence of MG132 StMKK1 accumulated to similar levels with and without PITG20303 (Fig. 7b). These results indicate that PITG20303 and PITG20300 may increase StMKK1 accumulation through inhibition of 26S proteasome-mediated degradation of StMKK1.

We further performed plasma membrane and nuclear protein isolation assays. The results showed that StMKK1 is also localized, although weakly, on the plasma membrane. The nuclear StMKK1 is not significantly stabilized by either PITG20303 or PITG20300, while the plasma membrane localization of StMKK1 is repressed strongly by PITG20303 and weakly by PITG20300, compared to the control (Fig. S13). To examine whether PITG20303 alters MAPK activation downstream of StMKK1, we transiently expressed GFP-MPK4 with either myc-GUS or myc-PITG20303 in *N. benthamiana* leaves and checked for activation of MPK4 protein upon flg22 treatment. The results showed that myc-MPK4, as well as MPK3/MPK6, are activated upon flg22 treatment, at 10 and 15 min following treatment (Fig. S14). However, PITG20303 does not affect MPK activation, as no clear differences were observed on MPK3/6/4 bands between *PITG20303*- and *GUS*-infiltrated leaves.

Discussion

The virulent variant of AVRblb2, *PITG20303*, was shown to be expressed in *P. infestans* isolates T30-4, 88069, 1306 and Pa21106 during potato infection (Haas *et al.*, 2009; Ah-Fong *et al.*, 2017; Yin *et al.*, 2017), and PITG20303 was secreted given that it was found in the secretome of *P. infestans* (Meijer *et al.*, 2014). In this study we demonstrate that PITG20303 localizes to the nucleus and the plasma membrane of the plant to promote pathogen colonization (Figs 1, S1, S2). PITG20303 and its avirulent variant PITG20300 all interact *in planta* with a potato defence negative regulator StMKK1 protein (Fig. 2). The consequence of this interaction is to promote *P. infestans* colonization and to suppress PTI responses (Figs 5, 6). We also provide evidence that PITG20303 and PITG20300 stabilize StMKK1, and

the virulence functions of nuclear-targeted PITG20303NLS and PITG20300NLS are dependent on StMKK1 (Figs 7, S12). There are seven paralogues of the Avrblb2 family (PITG04085, PITG04086, PITG20301, PITG20303, PITG18683, PITG04090, PITG20300) found in the genome of *P. infestans* T30-4 (Haas *et al.*, 2009), which forms four variants, in one of which a Phe residue at position 69 in the protein replaces the Ala/Ile/Val residue, in PITG20301 and PITG20303, resulting in a loss of recognition by its corresponding resistance gene *Rpi-blb2*. PITG20300 was reported to localize to the plasma membrane to target and inhibit the secretion of a host cysteine protease C14 (Bozkurt *et al.*, 2011). The presence of different variants of Avrblb2 in *P. infestans* isolates indicates the importance of the AVRblb2 effector family in pathogen virulence. Here we have demonstrated the novel function of the Avrblb2 family effector PITG20303 in supressing PTI immunity via interaction with the StMKK1 protein. Investigating the host target and virulence mechanism of Avrblb2 extends our knowledge of the roles of this important Avrblb2 family in *P. infestans* pathogenicity.

Subcellular localization assays show that both PITG20303 and PITG20300 show a nuclear and plasma membrane localization. However, PITG20303 localizes mainly to the nucleus and nuclear speckles, with weak signals on the plasma membrane, while PITG20300 localizes more on the plasma membrane, with weak signals in the nucleus and with no nuclear speckles found (Fig. S2). Plasma membrane/nuclear protein isolation assays further showed that for PITG20303 the proportion of nuclear- and plasma membrane-localized proteins is similar, being about 50% each. About 80% of PITG20300 is localized on the plasma membrane and only 16% is localized inside the nucleus (Figs S2, S3). Colocalization of these two effectors with StMKK1 showed that PITG20303 nicely colocalizes with StMKK1 in the nucleus, while PITG20300 weakly colocalizes with StMKK1 in the nucleus (Fig. S6). Both effectors were shown to interact with StMKK1 in Y2H, Co-IP and LCI assays (Figs 2, S5). In BiFC assays, PITG20303 interacts with StMKK1 in the nucleus, but the interaction was not observed for PITG20300 (Fig. 2). Because BiFC assays for PITG20303 and StMKK1 showed an interaction only in the host nucleus, the plasma membrane interaction is probably not sufficient to be detected by BiFC. PITG20300 localizes less in the nucleus than PITG20303 (Figs S2, S3), and thus the interaction of PITG20300 and StMKK1 is probably weaker than PITG20303 and StMKK1, leading to a failure of the interaction detected by the BiFC assay.

The fact that GFP-20303 and the nuclear targeted GFP-20303NLS/GFP-20300NLS partially or completely depends on NbMKK1 for suppression of ROS production and enhancement of infection while PITG20300 does not (Figs 6, S12) indicates that the nuclear localization of both effectors utilizes this interaction to repress plant PTI. PITG20303 probably has other host target proteins on the plasma membrane such as PITG20300, as the plasma membrane-localized myr-PITG20303 promotes pathogen colonization. Together, our results suggest that both PITG20303 and PITG20300 are likely to target multiple host proteins to modulate plant immunity. It is possible that they target plasma membrane-related proteins. This is similar to the *P. infestans* effector AVR3a, which was found to target and stabilize the E3-ligase CMPG1 (Bos *et al.*, 2010) and the cinnamyl alcohol dehydrogenase CAD7 (Li *et al.*, 2019).

The results presented here demonstrate that StMKK1 negatively regulates plant immunity to the late blight disease vector *P. infestans* by repressing plant PTI responses (Fig. 3). The role of MPK cascade proteins in plant immunity is rather complicated. For example, MEKK1-MKK1/2-MPK4 cascade proteins were reported as both positive (Zhang *et al.*, 2017) and negative regulators of plant defence. Cotton *GhMKK1* enhances plant susceptibility to the bacterial pathogen *Ralstonia solanacearum* (Lu *et al.*, 2013). Thus, we consider that StMKK1 might have additional roles in repressing plant immunity other than participating in MEKK1-MKK1/2-MPK4 cascade. It may participate in plant hormone biosynthesis or signalling pathways, as several MAPK cascade proteins were found to participate in salicylic acid (SA) signalling (Jagodzik *et al.*, 2018).

The constitutively activated StMKK1^{DE} interacts with both effectors and promotes pathogen colonization, while the kinase-deficient mutants StMKK1^{K99M} and StMKK1^{AA} have lost this ability (Fig. 4), indicating that the kinase activity of StMKK1 is required for PITG20303 interaction and plant defence repression. We also showed that without phosphorylation by the upstream kinase, StMKK1, but not StMKK1^{K99M}, phosphorylates StMPK4 (Fig. S11), suggesting that StMKK1 has self-phosphorylation activity and confirming that StMKK1 kinase activity is essential for effector interaction.
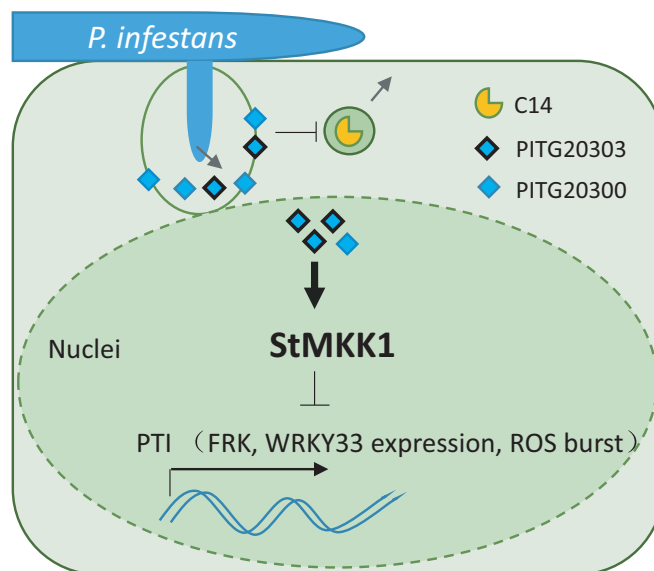

Fig. 8 *Phytophthora infestans* RXLR effector PITG20303 targets and stabilizes the potato StMKK1 protein. The model shows that upon *P. infestans* colonization, effectors PITG20300 and PITG20303 are secreted and translocated into the host cell, where PITG20300 inhibits the secretion of C14 at the plasma membrane. In the host nucleus these two effectors target and stabilize the potato StMKK1 protein to interfere with plant PTI. StMKK1 suppresses plant PTI responses, as indicated by the suppression of *FRK* and *WRKY33* expression and ROS burst.

MAPK cascades play essential roles in plant immunity, especially in plant PTI responses. Successful plant pathogens secret intracellular effectors to directly target MAPK cascade proteins to interfere with PTI (Eschen-Lippold *et al.*, 2016; Teper *et al.*, 2018; Hu *et al.*, 2019). Most of the effectors that target MAPK cascade components show a biochemical activity in regulating MAPK activity. In *Arabidopsis* the *mkk1/2* mutant shows an autoimmune phenotype mediated by the activation of a plant NB-LRR protein SUMM2, which senses the integrity of the MEKK1-MKK1/2-MPK4 cascade (Zhang *et al.*, 2012, 2017). Thus, interference of the MEKK1-MKK1/2-MPK4 cascade by pathogen effectors leads to the activation of SUMM2-mediated plant immunity, and that was true for *P. syringae* effector HopAI1 which inactivates MPK4 and triggers immunity when expressed in plants (Zhang *et al.*, 2012). In our case, although PITG20303 targets StMKK1, it neither triggered hypersensitive response or autoimmunity in *N. benthamiana* nor disturbed flg22-triggered MPK4 phosphorylation (Fig. S14). This indicates that PITG20303 does not disturb the MEKK1-MKK1/2-MPK4 kinase cascade, and thus does not trigger a SUMM2-mediated defence response. It is also possible that SUMM2 is missed in *N. benthamiana* plants.

PITG20303 suppresses plant immunity, as measured by *FRK* and *WRKY33* expression and ROS burst (Fig. 5), which is negatively regulated by its *in planta* interacting protein StMKK1. This indicates that *StMKK1* functions as a susceptibility gene that is targeted and modulated by the *P. infestans* effector PITG20303. However, how PITG20303 modulates StMKK1 is not fully clear. Here we showed that over-expression of the effectors PITG20303 and PITG20300 could stabilize the co-expressed StMKK1 protein. Further investigation into the effect of PITG20303 and PITG20300 on StMKK1 autophosphorylation or identifying and testing the effect of PITG20303 on the phosphorylation of StMKK1 substrate proteins in the suppression of plant immunity may help to answer this question.

In summary, we show that the AVRblb2 family effectors PITG20303 and PITG20300 target and stabilize a nuclear- and cytoplasmic-localized StMKK1 protein, and perturbs plant PTI responses that were negatively regulated by StMKK1 (Fig. 8). Furthermore, we have uncovered a role of StMKK1 in negative regulation of PTI responses by repressing the expression of *FRK* and *WRKY33* and ROS production. The kinase activity of StMKK1 is required for its repression of PTI, indicating it might have additional substrates *in planta* which are involved in plant immunity suppression. This research provides evidence that oomycete RXLR effectors can directly target an MAPK cascade protein and use it as a susceptibility gene to interfere with plant immunity. Our findings may help to identify novel plant susceptibility genes, and this knowledge may help to improve plant resistance to *Phytophthora* pathogens.

Author contributions

YD, YM and WS designed the research. YG, YD, XC, XZ, HZ, YM, GH and FL performed the experiments. YG and YD screened the Y2H library. YD and XC analysed the data. YD and WS wrote the manuscript with contributions from all authors. YD, XC and YG contributed equally to this work.

ORCID

Yu Du https://orcid.org/0000-0002-3512-0200
Weixing Shan https://orcid.org/0000-0001-7286-4041

References

Ah Fong AMV, Kim KS, Judelson HS. 2017. RNA-seq of life stages of the oomycete *Phytophthora infestans* reveals dynamic changes in metabolic, signal transduction, and pathogenesis genes and a major role for calcium signaling in development. *BMC Genomics* **18**: 198.

Berriri S, Garcia AV, Freidit Frey N, Rozhon W, Pateyron S, Leonhardt N, Montillet JL, Leung J, Hirt H, Colcombet J. 2012. Constitutively active Mitogen-activated protein kinase versions reveal functions of *Arabidopsis* MPK4 in pathogen defense signaling. *Plant Cell* **24**: 4281–4293.

Bi G, Zhou JM. 2017. MAP kinase signaling pathways: a hub of plant–microbe interactions. *Cell Host & Microbe* **21**: 270–273.

Boevink PC, Wang X, McLellan H, He Q, Naqvi S, Armstrong MR, Zhang W, Hein I, Gilroy EM, Tian Z et al. 2016. A *Phytophthora infestans* RXLR effector targets plant PP1c isoforms that promote late blight disease. *Nature Communications* **7**: 10311.

Bos JI, Armstrong MR, Gilroy EM, Boevink PC, Hein I, Taylor RM, Zhendong T, Engelhardt S, Vetukuri RR, Harrower B et al. 2010. *Phytophthora infestans* effector AVR3a is essential for virulence and manipulates plant immunity by stabilizing host E3 ligase CMPG1. *Proceedings of the National Academy of Sciences, USA* **107**: 9909–9914.

Bouwmeester K, de Sain M, Weide R, Gouget A, Klamer S, Canut H, Govers F. 2011. The lectin receptor kinase LecRK-I.9 is a novel *Phytophthora* resistance component and a potential host target for a RXLR effector. *PLoS Pathogens* **7**: e1001327.

Bozkurt TO, Schornack S, Win J, Shindo T, Ilyas M, Oliva R, Cano LM, Jones AM, Huitema E, van der Hoorn RA et al. 2011. *Phytophthora infestans* effector AVRblb2 prevents secretion of a plant immune protease at the haustorial interface. *Proceedings of the National Academy of Sciences, USA* **108**: 20832–20837.

Champouret N, Bouwmeester K, Rietman H, van der Lee T, Maliepaard C, Heupink A, van de Vondervoort PJ, Jacobsen E, Visser RG, van der Vossen EA et al. 2009. *Phytophthora infestans* isolates lacking class I *ipiO* variants are virulent on *Rpi-blb1* potato. *Molecular Plant–Microbe Interactions* **22**: 1535–1545.

Chen H, Zou Y, Shang Y, Lin H, Wang Y, Cai R, Tang X, Zhou JM. 2008. Firefly luciferase complementation imaging assay for protein-protein interactions in plants. *Plant Physiology* 146: 368–76.

Cheng BP, Yu XL, Ma ZC, Dong SM, Dou DL, Wang YC, Zheng XB. 2012. *Phytophthora sojae* effector Avh331 suppresses the plant defence response by disturbing the MAPK signalling pathway. *Physiological and Molecular Plant Pathology* 77: 1–9.

Cui HT, Wang YJ, Xue L, Chu JF, Yan CY, Fu JH, Chen MS, Innes RW, Zhou JM. 2010. *Pseudomonas syringae* effector protein AvrB perturbs *Arabidopsis* hormone signaling by activating MAP kinase 4. *Cell Host & Microbe* 7: 164–175.

Dagdas YF, Belhaj K, Maqbool A, Chaparro-Garcia A, Pandey P, Petre B, Tabassum N, Cruz-Mireles N, Hughes RK, Sklenar J *et al.* 2016. An effector of the Irish potato famine pathogen antagonizes a host autophagy cargo receptor. *eLife* 5: e10856.

Du Y, Berg J, Govers F, Bouwmeester K. 2015b. Immune activation mediated by the late blight resistance protein R1 requires nuclear localization of R1 and the effector AVR1. *New Phytologist* 207: 735–747.

Du Y, Mpina MH, Birch PR, Bouwmeester K, Govers F. 2015a. *Phytophthora infestans* RXLR effector AVR1 interacts with exocyst component Sec5 to manipulate plant immunity. *Plant Physiology* 169: 1975–1990.

Eschen-Lippold L, Jiang XY, Elmore JM, Mackey D, Shan LB, Coaker G, Scheel D, Lee J. 2016. Bacterial AvrRpt2-like cysteine proteases block activation of the *Arabidopsis* Mitogen-activated protein kinases, MPK4 and MPK11. *Plant Physiology* 171: 2223–2238.

Fan G, Yang Y, Li T, Lu W, Du Y, Qiang X, Wen Q, Shan W. 2018. A *Phytophthora capsici* RXLR effector targets and inhibits a plant PPIase to suppress endoplasmic reticulum-mediated immunity. *Molecular Plant* 11: 1067–1083.

Feng F, Yang F, Rong W, Wu X, Zhang J, Chen S, He C, Zhou JM. 2012. A *Xanthomonas* uridine 5′-monophosphate transferase inhibits plant immune kinases. *Nature* 485: 114–118.

Haas BJ, Kamoun S, Zody MC, Jiang RHY, Handsaker RE, Cano LM, Grabherr M, Kodira CD, Raffaele S, Torto-Alalibo T *et al.* 2009. Genome sequence and analysis of the Irish potato famine pathogen *Phytophthora infestans*. *Nature* 461: 393–398.

Hardham AR, Cahill DM. 2010. The role of oomycete effectors in plant–pathogen interactions. *Functional Plant Biology* 37: 919–925.

Haverkort AJ, Boonekamp PM, Hutten R, Jacobsen E, Lotz LAP, Kessel GJT, Vossen JH, Visser RGF. 2016. Durable late blight resistance in potato through dynamic varieties obtained by cisgenesis: scientific and societal advances in the DuRPh Project. *Potato Research* 59: 35–66.

He P, Shan L, Lin NC, Martin GB, Kemmerling B, Nurnberger T, Sheen J. 2006. Specific bacterial suppressors of MAMP signaling upstream of MAPKKK in *Arabidopsis* innate immunity. *Cell* 125: 563–575.

He Q, Naqvi S, McLellan H, Boevink PC, Champouret N, Hein I, Birch PRJ. 2018. Plant pathogen effector utilizes host susceptibility factor NRL1 to degrade the immune regulator SWAP70. *Proceedings of the National Academy of Sciences, USA* 115: E7834–E7843.

Hu T, Huang C, He Y, Castillo-Gonzalez C, Gui X, Wang Y, Zhang X, Zhou X. 2019. βC1 protein encoded in geminivirus satellite concertedly targets MKK2 and MPK4 to counter host defense. *PLoS Pathogens* 15: e1007728.

Ingle RA, Carstens M, Denby KJ. 2006. PAMP recognition and the plant–pathogen arms race. *BioEssays* 28: 880–889.

Jagodzik P, Tajdel-Zielinska M, Ciesla A, Marczak M, Ludwikow A. 2018. Mitogen-activated protein kinase cascades in plant hormone signaling. *Frontiers in Plant Science* 9: 1387.

Jing M, Guo B, Li H, Yang B, Wang H, Kong G, Zhao Y, Xu H, Wang Y, Ye W *et al.* 2016. A *Phytophthora sojae* effector suppresses endoplasmic reticulum stress-mediated immunity by stabilizing plant binding immunoglobulin proteins. *Nature Communications* 7: 11685.

Jones JDG, Dangl JL. 2006. The plant immune system. *Nature* 444: 323–329.

Kale SD, Gu B, Capelluto DGS, Dou D, Feldman E, Rumore A, Arredondo FD, Hanlon R, Fudal I, Rouxel T *et al.* 2010. External lipid PI3P mediates entry of eukaryotic pathogen effectors into plant and animal host cells. *Cell* 142: 284–295.

King SR, McLellan H, Boevink PC, Armstrong MR, Bukharova T, Sukarta O, Win J, Kamoun S, Birch PR, Banfield MJ. 2014. *Phytophthora infestans* RXLR

effector PexRD2 interacts with host MAPKKK epsilon to suppress plant immune signaling. *Plant Cell* 26: 1345–1359.

Kong L, Qiu XF, Kang JG, Wang Y, Chen H, Huang J, Qiu M, Zhao Y, Kong GH, Ma ZC *et al.* 2017. A *Phytophthora* effector manipulates host histone acetylation and reprograms defense gene expression to promote infection. *Current Biology* 27: 981–991.

Li B, Jiang S, Yu X, Cheng C, Chen S, Cheng Y, Yuan JS, Jiang D, He P, Shan L. 2015. Phosphorylation of trihelix transcriptional repressor ASR3 by MAP KINASE4 negatively regulates *Arabidopsis* immunity. *Plant Cell* 27: 839–856.

Li L, Kim P, Yu L, Cai G, Chen S, Alfano JR, Zhou JM. 2016. Activation-dependent destruction of a co-receptor by a *Pseudomonas syringae* effector dampens plant immunity. *Cell Host & Microbe* 20: 504–514.

Li T, Wang Q, Feng R, Li L, Ding L, Fan G, Li W, Du Y, Zhang M *et al.* 2019. Negative regulators of plant immunity derived from cinnamyl alcohol dehydrogenases are targeted by multiple *Phytophthora* Avr3a-like effectors. *New Phytologist*. doi: 10.1111/nph.16139.

Li X, Zhang Y, Huang L, Ouyang Z, Hong Y, Zhang H, Li D, Song F. 2014. Tomato SlMKK2 and SlMKK4 contribute to disease resistance against *Botrytis cinerea*. *BMC Plant Biology* 14: 166.

Ling TF, Bellin D, Vandelle E, Imanifard Z, Delledonne M. 2017. Host-mediated S-Nitrosylation disarms the bacterial effector HopAI1 to reestablish immunity. *Plant Cell* 29: 2871–2881.

Long Y, Xie D, Zhao Y, Shi D, Yang W. 2019. BICELLULAR POLLEN 1 is a modulator of DNA replication and pollen development in *Arabidopsis*. *New Phytologist* 222: 588–603.

Lu W, Chu X, Li Y, Wang C, Guo X. 2013. Cotton GhMKK1 induces the tolerance of salt and drought stress, and mediates defence responses to pathogen infection in transgenic *Nicotiana benthamiana*. *PLoS One* 8: e68503.

Lu X, Xiong Q, Cheng T, Li QT, Liu XL, Bi YD, Li W, Zhang WK, Ma B, Lai YC *et al.* 2017. A PP2C-1 allele underlying a quantitative trait locus enhances soybean 100-seed weight. *Molecular Plant* 10: 670–684.

McLellan H, Boevink PC, Armstrong MR, Pritchard L, Gomez S, Morales J, Whisson SC, Beynon JL, Birch PR. 2013. An RXLR effector from *Phytophthora infestans* prevents re-localisation of two plant NAC transcription factors from the endoplasmic reticulum to the nucleus. *PLoS Pathogens* 9: e1003670.

Meijer HJG, Mancuso FM, Espadas G, Seidl MF, Chiva C, Govers F, Sabido E. 2014. Profiling the secretome and extracellular proteome of the potato late blight pathogen *Phytophthora infestans*. *Molecular & Cellular Proteomics* 13: 2101–2113.

Murphy F, He Q, Armstrong M, Giuliani LM, Boevink PC, Zhang W, Tian Z, Birch PRJ, Gilroy EM. 2018. The potato MAP3K StVIK is required for the *Phytophthora infestans* RXLR effector Pi17316 to promote disease. *Plant Physiology* 177: 398–410.

Oliva RF, Cano LM, Raffaele S, Win J, Bozkurt TO, Belhaj K, Oh SK, Thines M, Kamoun S. 2015. A recent expansion of the RXLR effector gene *Avrblb2* is maintained in global populations of *Phytophthora infestans* indicating different contributions to virulence. *Molecular Plant–Microbe Interactions* 28: 901–912.

Qiao Y, Shi J, Zhai Y, Hou Y, Ma W. 2015. *Phytophthora* effector targets a novel component of small RNA pathway in plants to promote infection. *Proceedings of the National Academy of Sciences, USA* 112: 5850–5855.

Ren Y, Armstrong M, Qi Y, McLellan H, Zhong C, Du B, Birch PRJ, Tian Z. 2019. *Phytophthora infestans* RXLR effectors target parallel steps in an immune signal transduction pathway. *Plant Physiology* 180: 2227–2239.

Saunders DGO, Breen S, Win J, Schornack S, Hein I, Bozkurt TO, Champouret N, Vleeshouwers VGAA, Birch PRJ, Gilroy EM *et al.* 2012. Host protein BSL1 associates with *Phytophthora infestans* RXLR effector AVR2 and the *Solanum demissum* immune receptor R2 to mediate disease resistance. *Plant Cell* 24: 3420–3434.

Tameling WIL, Baulcombe DC. 2007. Physical association of the NB-LRR resistance protein Rx with a Ran GTPase-activating protein is required for extreme resistance to Potato virus X. *Plant Cell* 19: 1682–1694.

Teper D, Girija AM, Bosis E, Popov G, Savidor A, Sessa G. 2018. The *Xanthomonas euvesicatoria* type III effector XopAU is an active protein kinase that manipulates plant MAP kinase signaling. *PLoS Pathogens* 14: e1006880.

Tomczynska I, Stumpe M, Mauch F. 2018. A conserved RXLR effector interacts with host RABA-type GTPases to inhibit vesicle-mediated secretion of antimicrobial proteins. *The Plant Journal* 95: 187–203.

Turnbull D, Yang L, Naqvi S, Breen S, Welsh L, Stephens J, Morris J, Boevink PC, Hedley PE, Zhan J *et al.* 2017. RXLR effector AVR2 up-regulates a brassinosteroid responsive bHLH transcription factor to suppress immunity. *Plant Physiology* 174: 356–369.

Ueno Y, Yoshida R, Kishi-Kaboshi M, Matsushita A, Jiang CJ, Goto S, Takahashi A, Hirochika H, Takatsuji H. 2015. Abiotic stresses antagonize the rice defence pathway through the tyrosine-dephosphorylation of OsMPK6. *PLoS Pathogens* 11: e1005231.

Vetukuri RR, Whisson SC, Grenville-Briggs LJ. 2017. *Phytophthora infestans* effector Pi14054 is a novel candidate suppressor of host silencing mechanisms. *European Journal of Plant Pathology* 149: 771–777.

Vleeshouwers VGAA, Raffaele S, Vossen JH, Champouret N, Oliva R, Segretin ME, Rietman H, Cano LM, Lokossou A, Kessel G *et al.* 2011. Understanding and exploiting late blight resistance in the age of effectors. *Annual Review of Phytopathology* 49: 507–531.

Wang X, Boevink P, McLellan H, Armstrong M, Bukharova T, Qin Z, Birch PR. 2015. A host KH RNA-binding protein is a susceptibility factor targeted by an RXLR effector to promote late blight disease. *Molecular Plant* 8: 1385–1395.

Wang YJ, Li JF, Hou SG, Wang XW, Li YA, Ren DT, Chen S, Tang XY, Zhou JM. 2010. A *Pseudomonas syringae* ADP-ribosyltransferase inhibits *Arabidopsis* mitogen-activated protein kinase kinases. *Plant Cell* 22: 2033–2044.

Yang KY, Liu YD, Zhang SQ. 2001. Activation of a mitogen-activated protein kinase pathway is involved in disease resistance in tobacco. *Proceedings of the National Academy of Sciences, USA* 98: 741–746.

Yang L, McLellan H, Naqvi S, He Q, Boevink PC, Armstrong M, Giuliani LM, Zhang W, Tian Z, Zhan J *et al.* 2016. Potato NPH3/RPT2-like protein StNRL1, targeted by a *Phytophthora infestans* RXLR effector, is a susceptibility factor. *Plant Physiology* 171: 645–657.

Yin JL, Gu B, Huang GY, Tian Y, Quan JL, Lindqvist-Kreuze H, Shan WX. 2017. Conserved RXLR effector genes of *Phytophthora infestans* expressed at the early stage of potato infection are suppressive to host defense. *Frontiers in Plant Science* 8: 2155.

Zhang J, Li W, Xiang T, Liu Z, Laluk K, Ding X, Zou Y, Gao M, Zhang X, Chen S *et al.* 2010. Receptor-like cytoplasmic kinases integrate signaling from multiple plant immune receptors and are targeted by a *Pseudomonas syringae* effector. *Cell Host & Microbe* 7: 290–301.

Zhang J, Shao F, Li Y, Cui H, Chen L, Li H, Zou Y, Long C, Lan L, Chai J *et al.* 2007. A *Pseudomonas syringae* effector inactivates MAPKs to suppress PAMP-induced immunity in plants. *Cell Host & Microbe* 1: 175–185.

Zhang Z, Wu Y, Gao M, Zhang J, Kong Q, Liu Y, Ba H, Zhou J, Zhang Y. 2012. Disruption of PAMP-induced MAP kinase cascade by a *Pseudomonas syringae* effector activates plant immunity mediated by the NB-LRR protein SUMM2. *Cell Host & Microbe* 11: 253–263.

Zhang ZB, Liu YN, Huang H, Gao MH, Wu D, Kong Q, Zhang YL. 2017. The NLR protein SUMM2 senses the disruption of an immune signaling MAP kinase cascade via CRCK3. *EMBO Reports* 18: 292–302.

Zheng X, McLellan H, Fraiture M, Liu X, Boevink PC, Gilroy EM, Chen Y, Kandel K, Sessa G, Birch PR *et al.* 2014. Functionally redundant RXLR effectors from *Phytophthora infestans* act at different steps to suppress early flg22-triggered immunity. *PLoS Pathogens* 10: e1004057.

Zheng X, Wagener N, McLellan H, Boevink PC, Hua C, Birch PRJ, Brunner F. 2018. *Phytophthora infestans* RXLR effector SFI5 requires association with calmodulin for PTI/MTI suppressing activity. *New Phytologist* 219: 1433–1446.

Zhou J, Wu S, Chen X, Liu C, Sheen J, Shan L, He P. 2014. The *Pseudomonas syringae* effector HopF2 suppresses *Arabidopsis* immunity by targeting BAK1. *The Plant Journal* 77: 235–245.

Zipfel C. 2008. Pattern-recognition receptors in plant innate immunity. *Current Opinion in Immunology* 20: 10–16.

Supporting Information

Additional Supporting Information may be found online in the Supporting Information section at the end of the article.

Fig. S1 PITG20303 promotes plant susceptibility to *Phytophthora parasitica*.

Fig. S2 Subcellular localization of PITG20303 and PITG20300.

Fig. S3 Plasma membrane and nuclear protein isolation assays.

Fig. S4 *PITG20303* promotes *P. infestans* colonization at different subcellular localizations.

Fig. S5 Both PITG20303 and PITG20300 interact with StMKK1 and SlMKK1.

Fig. S6 StMKK1 colocalizes with the effector PITG20303 in the nucleus of plant cells.

Fig. S7 Phylogenetic tree of MKK1/2 proteins from Arabidopsis, rice, *Populus*, tomato, potato and *N. benthamiana*.

Fig. S8 Sequence alignment of MKK1 from *N. benthamiana*, tomato and potato.

Fig. S9 Sequence alignment of TRV-*MKK1* and *NbMKK1* genes.

Fig. S10 Silencing efficiency and plant morphology of *N. benthamiana* plants inoculated with TRV-*MKK1*.

Fig. S11 The *in vitro* phosphorylation assays.

Fig. S12 NbMKK1 is required for virulence activities of GFP-PITG20303NLS and GFP-PITG20300NLS.

Fig. S13 The plasma membrane-localized StMKK1 was reduced by PITG20303 and PITG20300.

Fig. S14 Western blots showing the effect of PITG20303 on MAPK kinase activities.

Table S1 Primers used in this study.

Please note: Wiley Blackwell are not responsible for the content or functionality of any Supporting Information supplied by the authors. Any queries (other than missing material) should be directed to the *New Phytologist* Central Office.